# Reversible Nanoparticle-Micelle Transformation of Ionic Liquid-Sulfonatocalix[6]arene Aggregates

| | |
|---|---|
| Journal: | *Langmuir* |
| Manuscript ID: | Draft |
| Manuscript Type: | Article |
| Date Submitted by the Author: | n/a |
| Complete List of Authors: | Wintgens, Veronique; Laboratoire de Recherche sur les Polymeres, LRP-CNRS<br>Miskolczy, Zsombor; Chemical Research Center, Hungarian Academy of Sciences,<br>Guigner, Jean-Michel; Université Pierre et Marie Curie, Institut de Minéralogie et Physique des Milieux Condensés<br>Amiel, Catherine; University Paris 12 Val de Marne, Laboratoire de Recherche sur les Polymeres<br>Harangozó, József; Research Centre for Natural Sciences, Hungarian Academy of Sciences, Institute of Materials and Environmental Chemistry<br>Biczók, László; Research Centre for Natural Sciences, Hungarian Academy of Sciences, Institute of Materials and Environmental Chemistry |
| | |

# Reversible Nanoparticle–Micelle Transformation of Ionic Liquid–Sulfonatocalix[6]arene Aggregates

**Véronique Wintgens,[a] Zsombor Miskolczy,[c] Jean-Michel Guigner,[b] Catherine Amiel,[a] József G. Harangozó,[c] László Biczók[c*]**

[a]*Université Paris Est, ICMPE (UMR7182), CNRS, UPEC, F 94320 Thiais, France*

[b]*Institut de Minéralogie et de Physique des Milieux Condensés, IMPMC, Université Pierre et Marie Curie, CNRS, 4 Place Jussieu, 75005 Paris, France*

[c]*Institute of Materials and Environmental Chemistry, Research Centre for Natural Sciences, Hungarian Academy of Sciences, P.O. Box 286, 1519 Budapest, Hungary*

[*] Corresponding author. Phone: (+36 1) 382-6614; E-mail: biczok.laszlo@ttk.mta.hu

**Abstract**

The effect of temperature and NaCl concentration variations on the self-assembly of 1-methyl-3-tetradecylimidazolium ($C_{14}mim^+$) and 4-sulfonatocalix[6]arene (SCX6) was studied by dynamic light scattering and isothermal calorimetric methods at pH 7. Inclusion complex formation promoted the self-assembly to spherical nanoparticles (NP), which transformed to supramolecular micelles (SM) in the presence of NaCl. Highly reversible, temperature-responsive behavior was observed, and the conditions of the NP–SM transition could be tuned by the alteration of $C_{14}mim^+$:SCX6 mixing ratio and NaCl concentration. The association to SM was always exothermic with enthalpy independent on the amount of NaCl. In contrast, NPs were produced in endothermic process at low temperature, and the enthalpy change became less favorable upon increase of NaCl concentration. The NP formation was accompanied by negative molar heat capacity change, which further diminished when NaCl concentration was raised.

*Key words:* Nanoparticle, supramolecular interaction, self-assembly, macrocycle, surfactant

## 1. INTRODUCTION

Supramolecular amphiphiles, the surfactants composed of noncovalently bound constituents, have their versatile applications and easily tunable properties.[1-3] Host-guest complex formation with macrocyclic compounds was often used to alter the thermodynamics of association and the morphology of the product. Inclusion of a surfactant in the cavity of cyclodextrins usually increases the critical micelle concentration.[4] The confinement of the dominant component of mixed cationic–anionic surfactant systems in β-cyclodextrin promoted aggregate growth leading to micelle-to-vesicle transition.[5] Spontaneous formation of giant vesicles was found upon coinclusion of methylviologen substituted with a long alkyl chain and 2,6-dihydroxynaphthalene inside cucurbit[8]uril.[6] This host induced vesicle formation by ternary complex formation with pyrene-functionalized peptide and N-methyl-N'-octadecyl viologen.[7] The dynamic character of noncovalent interactions was exploited to create stimuli-responsive self-assembled systems. Cyclodextrins were most frequently used as host macrocycles in associates exhibiting structure alteration controllable by pH,[8] redox reaction,[9] temperature[10] or photoirradiation.[11,12]

Because of their flexible π-electron-rich cavity and negative charge, 4-sulfonatocalix[n]arenes (SCXn) are particularly beneficial building elements for the creation of diverse nanostructures.[13-15] The role of SCXn in the design of fluorescent sensing systems, pesticide detoxification, drug delivery,[16] biochemistry,[17,18] crystal engineering[13,19] and supramolecular polymerization[20] has been reviewed. In contrast to cyclodextrins or cucurbiturils, which induces the dissociation of aggregates by host-guest complexation,[21] the binding to SCXn promotes the aggregation of aromatic or amphiphilic compounds.[22-25] We have demonstrated the inclusion of 1-alkyl-3-methylimidazolium ($C_nmim^+$) type of ionic liquids in SCXn[26] and unraveled the alteration of the binding thermodynamics with the length of the 1-alkyl substituent on the methylimidazolium moiety.[27,28] When the aliphatic

chain was composed of n = 12, 14 or 16 C atoms, $C_n mim^+$ cations and SCX6 spontaneously organized to spherical nanoparticles (NPs) possessing dense multilayered structure and 7:1 stoichiometry.[29] The main objectives of the present work were to demonstrate the stimuli-responsive behavior of these NPs, and to reveal the major factors affecting their thermal-induced structural change. We focus on the self-assembly of $C_{14}mim^+$ and SCX6 (Scheme 1) in solutions neutralized by NaOH.

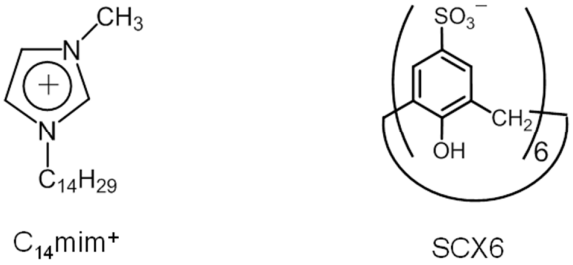


**Scheme 1.** Formulas of ionic liquid cation and 4-sulfonatocalix[6]arene

## 2. EXPERIMENTAL SECTION

**Materials.** 1-Methyl-3-tetradecyl-imidazolium bromide ($C_{14}mim^+Br^-$) was synthesized by the previously published procedure.[30] 4-Sulfonatocalix[6]arene (SCX6) (Acros Organics) contained 1:13 stoichiometric amount of water in its crystal structure.[31] SCX6 solutions were always neutralized by the minimum volume of concentrated NaOH. Water of ultrapure quality was used as solvent. 2-Hydroxy-substituted Nile Red (HONR), also called 9-diethylamino-2-hydroxy-5*H*-benz[*a*]phenoxazin-5-one (Aldrich) was employed without further purification.

**Sample preparation.** Stock solutions of $C_{14}mim^+Br^-$ (2 mM) and SCX6 (1 mM, pH 7) were prepared. NPs were obtained by mixing the required amounts of these solutions under stirring at 150 rpm at 25°C. SCX6 concentration was kept constant (0.1 mM) unless otherwise noted. Ionic strength was varied by addition of small volume (<50 μl) of concentrated solution of NaCl. The solutions were usually equilibrated 200 min at 25°C before measurements.

**Utilization of fluorescent probe.** 23 nmol HONR in methanol was added to 5 ml flask and the solvent was evaporated by letting nitrogen flow over the solution. After adding the supramolecular surfactant aqueous solution, the sample was equilibrated for 2 days in the dark.

**Instrumentation.** The absorption spectra were recorded on an Agilent Technologies Cary60 spectrophotometer. Particle size was determined by dynamic light scattering on a Zetasizer Nano-ZS (Malvern Instrument) equipped with a He-Ne laser ($\lambda$ = 633 nm, scattering angle 173°). Each measurement was the average of 12 runs of 10 seconds. Data were analyzed with the software developed by the manufacturer using a distribution analysis (General Purpose analysis). The mean diameter of the NPs was calculated on the basis of number distribution. Experiment was repeated at least twice. NPs were separated from the liquid phase by an ultracentrifuge from Beckman Coulter (Optima Max-XP, type TLA 110 rotor). Total carbon analyses were performed on a Shimadzu TOC-L CSN instrument, which was calibrated by a potassium hydrogen phthalate solution in ultrapure water (2.125 g $dm^{-3}$ corresponding to 1000 mgC $dm^{-3}$). ITC measurements were carried out with a MicroCal VP-ITC microcalorimeter. 10 μl of 3.4 mM ionic liquid solutions were injected from the computer controlled microsyringe at an interval of 180 s into the cell (volume = 1.4569 ml) containing 0.1 mM SCX6 solution at pH 7, while stirring at 450 rpm. Cryo-TEM images were taken on an Ultrascan 2 k CCD camera (Gatan, USA), using a $LaB_6$ JEOL JEM 2100 (JEOL, Japan) cryo-microscope operating at 200 kV with a JEOL low dose system (Minimum Dose System, MDS) to protect the thin ice film from any irradiation before imaging and to reduce the irradiation during the image capture. The images were recorded at 93 K and digitally corrected using the ImageJ software. The samples were prepared as follows. A drop of the suspension was deposited on a Quantifoil grid (Micro Tools GmbH, Germany). The excess of solution was then blotted out with a filter paper, and before evaporation the grid was

quench-frozen in liquid ethane to form a thin vitreous ice film. The grid was mounted in a Gatan 626 cryo-holder cooled with liquid nitrogen and transferred in the microscope.

## 3. RESULTS

**NaCl-promoted NP–micelle transition.** In accordance with previous findings in acidic solutions,[29] NPs of negative ζ potential were produced when $C_{14}mim^+$ was added to the neutralized solution of 0.1 mM SCX6 in 6 - 2 molar excess at 298 K. The initial points in Figure 1 and Supporting Information Figure S1 demonstrate that the NP size (d ~ 60 nm) is independent on the $C_{14}mim^+$:SCX6 molar ratio (r) in the absence of NaCl. However, the gradual increase of NaCl concentration in mixtures of different r brought about two types of

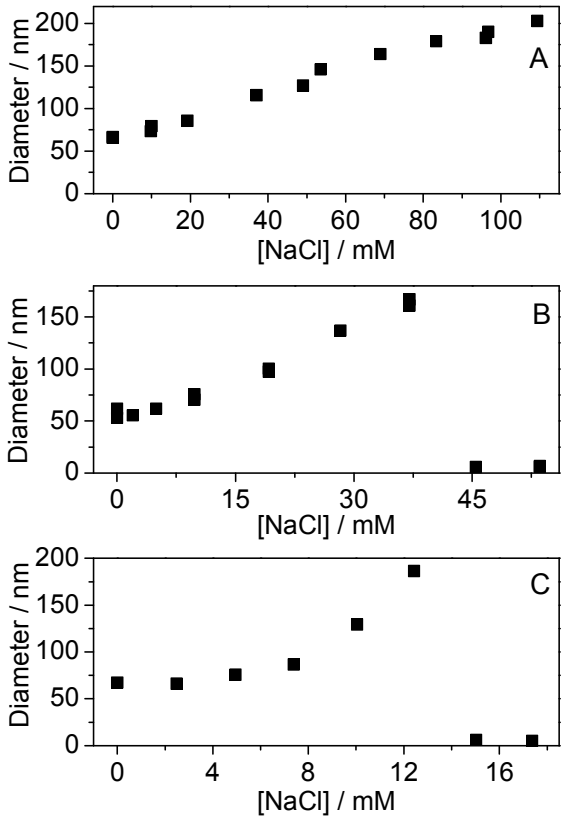


**Figure 1.** Mean particle diameter as a function of NaCl concentration for $C_{14}mim^+$:SCX6 solution of molar ratio (A) 6 (B) 4 and (C) 2 at 298 K. Measurement was performed immediately after each successive NaCl addition. [SCX6] = 0.1 mM

behaviors. At r = 5 - 6, the initial mean NP diameter steadily increased until a fast coalescence occurred around 150 mM NaCl concentration. Contrarily, NP size growth followed by a sudden considerable size diminution was observed at $2 \leq r \leq 4$. The abrupt structure change took place around 40, 25, and 15 mM NaCl concentration in the case of r = 4, 3, and 2, respectively. This phenomenon was attributed to the reassembly of the NP components to supramolecular micelles (SM) of 6.0 ± 0.3 nm mean diameter. When *r* is low, smaller number of SM is produced at constant SCX6 concentration. Consequently, less NaCl can ensure SM formation, and the NP–SM transition occurs at lower NaCl concentration. The SM size did not vary significantly under our experimental conditions. In the absence of SCX6, micelles of 4.5 ± 0.3 nm mean diameter was found in 2.5 mM $C_{14}mim^{+}Br^{-}$ and 20 mM NaCl solution at 298 K and 277 K alike. The larger size of SM could indicate the incorporation of SCX6 macrocycles. NPs formed at $r \leq 6$ are negatively charged because the outer layer of the NPs is mainly composed of SCX6.[29] For example, the zeta potential (ζ) is –43 mV or –60 mV for NPs formed at r = 3 without or with 15 mM NaCl, respectively. The more negative ζ in the presence of NaCl probably arises from the NP size increase. NPs coalesced quickly at r = 8 due to a ζ value close to zero, whereas positively charged NPs were produced at $r \geq 9$ because the outer layer of NPs is composed mainly of $C_{14}mim^{+}$ at large excess of ionic liquid over SCX6. The addition of at least 50 and 70 mM NaCl brought about precipitation at r = 12 - 15 and r = 18, respectively.

**Thermal-induced reversible SM–NP interconversion.** At constant $C_{14}mim^{+}$:SCX6 molar ratio, the onset temperature of SM–NP transformation can be tuned by the variation of NaCl concentration. Figure 2 displays the results achieved in the solution of 0.2 mM $C_{14}mim^{+}$ and 0.1 mM SCX6. The SMs were stable till higher temperature when more NaCl was added to the solution, and NPs were not produced below 300 and 306 K in the presence of 15 and 50

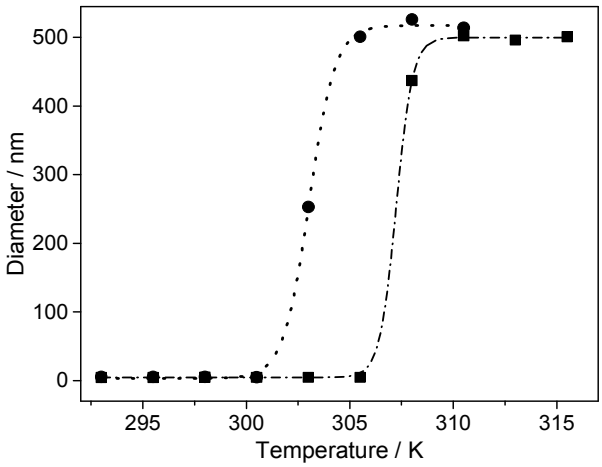


**Figure 2.** Effect of NaCl addition on the particle mean diameter at various temperatures for $C_{14}mim^+$:SCX6 solution of molar ratio 2 with 15 mM NaCl (●) and 50 mM NaCl (■). [SCX6] = 0.1 mM.

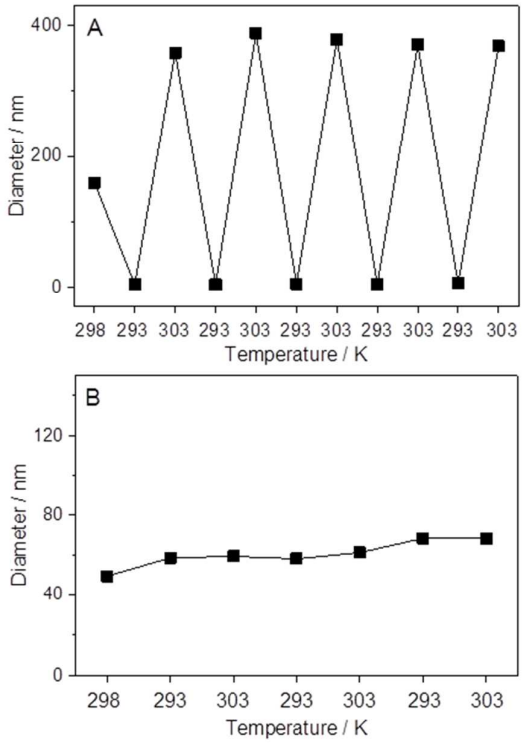


**Figure 3.** (A) Mean diameter of particles for $C_{14}mim^+$:SCX6 solution of molar ratio 3 with 15mM NaCl measured 20 min after repeated switch of temperature between 293 and 303 K. (B) Results of an analogous experiment in the absence of NaCl. [SCX6] = 0.1 mM

mM NaCl concentrations, respectively. Above these temperatures, the initial growth of NPs leveled off. The type of aggregates produced by self-assembly could be controlled by temperature. As a representative example, Figure 3A presents how the cycling of temperature between 293 and 303 K influenced the mean particle diameter (d). The initial NPs of d = 160 nm vanished upon cooling to 293 K, and SMs of 6 nm diameter emerged. The temperature rise to 303 K resulted in NP solution (d = 370 nm). The size of aggregates was constant within the limits of experimental errors even after several temperature variation cycles. Similar NP–SM interconversion was observed at $[C_{14}mim^+]/[SCX6]$ = 2 or 4. At reactant ratio 2, NP–SM transformations were observed at temperature alteration between 298 and 303 K, whereas switching between 293 and 298 K was needed at $[C_{14}mim^+]/[SCX6]$ = 4. Noteworthily, no thermal-induced SM formation occurred in the absence of NaCl in the 293-303 K temperature range (Figure 3B).

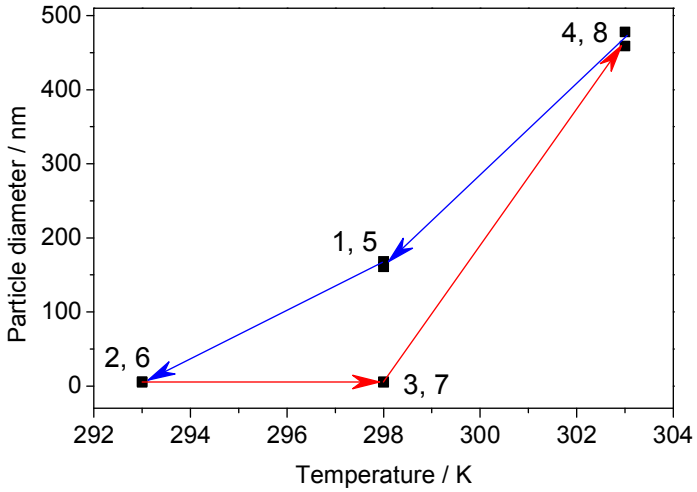


**Figure 4.** Mean particle diameter for $C_{14}mim^+$:SCX6 solution of molar ratio 3 with 15 mM NaCl after 40 min equilibration time. The temperature was changed in the order of the numbers as shown by the arrows. [SCX6] = 0.1 mM

Repeating the experiment whose results are presented in Figure 3A using temperature intervals of 5 K, a hysteresis was found that remained even when 40 min equilibration time was employed (Figure 4). This indicates that the rearrangement of SMs into NPs is slower than the reverse process.

**Stoichiometry of the components in NPs.** The amounts of the components in the NPs were obtained as a difference between the total concentrations and the concentrations in the aqueous phase. The NPs were separated from the solutions by ultracentrifugation, and the supernatants were analyzed by total carbon content measurement and spectrophotometric determination of SCX6 concentration as previously described.[29] In the mixture of 0.4 mM $C_{14}mim^+$ and 0.1 mM SCX6 at 298 K, $C_{14}mim^+$:SCX6 molar ratio in NPs were found to be 7.4 ± 0.5 and 7.2 ± 0.5 at [NaCl] = 0 and 15 mM, respectively. These values indicate that the presence of 15 mM NaCl insignificantly modified the stoichiometry of association although it induced a slight increase in the NP diameter (Figure 1B).

**Nanoparticle Structure.** The morphology of the NPs was characterized by cryo-TEM and as a representative example, we studied the NPs at molar ratio of 4 (Figure 5A-C) and the corresponding SMs obtained after adding 53 mM NaCl into the NPs suspension (Figure 5D). The observed NPs are spherical with diameter varying between 45 and 120 nm. The average diameter is around 71 ± 20 nm from 45 measurements, which is in agreement with the results of the DLS studies. Few smaller aggregates (d ~ 7 nm) are also observed (Figure 5A-B), corresponding to SMs. Interestingly, NPs show internal structure (Figure 5C). The core of the NPs exhibits parallel lines made of smaller units suggesting lamellar structure for the NP core; each unit has a size around 2 nm and could correspond to one SCX6 associated with 7 $C_{14}mim^+$. An amorphous shell of 10-12 nm appears around the structured core. The image of

the SMs at ratio 4 shows many well-separated aggregates inside the thin vitreous ice film (Figure 5D). The SMs are spherical with diameters mainly below 15 nm in accordance with the DLS results. Among the numerous images recorded for this sample, it should be noted that no NPs were observed.

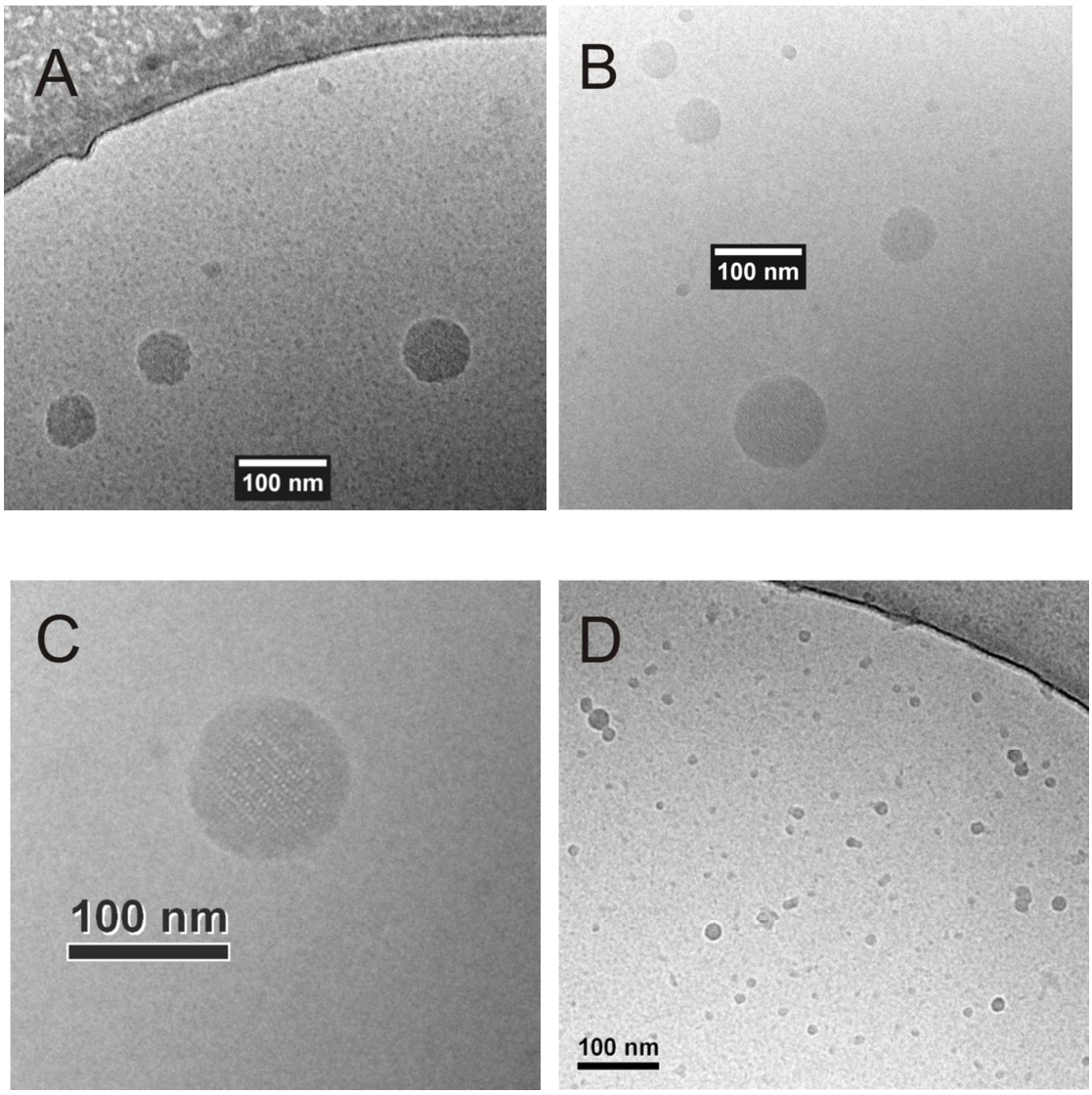


**Figure 5** Cryo-TEM images of (A-C) $C_{14}mim^+$:SCX6 solution of molar ratio 4 and (D) $C_{14}mim^+$:SCX6 solution of molar ratio 4 with 53 mM NaCl. [SCX6] = 0.2 mM.

**Critical aggregation concentration (cac) of supramolecular micelle.** The solubility enhancement of 2-hydroxy-substituted Nile Red (HONR, Scheme 2), a highly fluorescent, solvatochromic dye[32] has been successfully employed as an environmental sensitive fluorescent probe for the determination of critical micelle concentration of ionic liquids.[30,33]

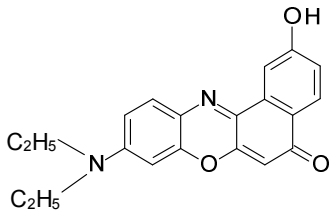


HONR

**Scheme 2** Formula of 2-hydroxy-substituted Nile Red fluorescent probe

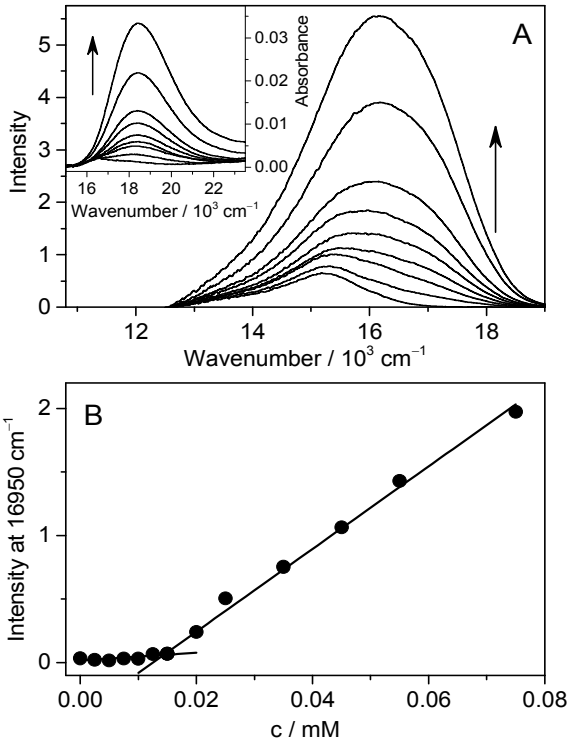


**Figure 6.** (A) Alteration of fluorescence and absorption (inset) spectra for saturated HONR solutions of $C_{14}mim^+$:SCX6 (molar ratio 2) and 50 mM NaCl at pH 7 ([$C_{14}mim^+$] = 0, 0.02, 0.025, 0.035, 0.045, 0.055, 0.075, 0.0135, and 0.175 mM). Temperature was 296 K. Excitation took place at 510 nm. (B) Fluorescence intensity at 16950 $cm^{-1}$ as a function of $C_{14}mim^+$ concentration at $C_{14}mim^+$:SCX6 molar ratio of 2 in 50 mM NaCl solution at pH 7.

Its solubility is very low in water and SCX6 aqueous solution, but significantly grows upon binding to micelles. Figure 6A displays the change of the fluorescence and absorption (inset) spectra upon parallel increase of the $C_{14}mim^+$ and SCX6 concentration keeping their molar ratio r = 2 in 50 mM NaCl solution. The HONR spectra remain unaltered up to 0.015 mM $C_{14}mim^+$ concentration because neither $C_{14}mim^+$ nor SCX6 enhance HONR solubility in this concentration range. However, further increase of the amounts of additives leads to SM formation. As the number of SMs grows, more HONR can be encapsulated and the absorbance and the fluorescence intensity gradually grow. Figure 6B clearly shows a break in the plot of the fluorescence intensity at 590 nm vs $C_{14}mim^+$ concentration. From the location of the abrupt intensity enhancement, a value of 0.015 mM is obtained for the cac of $C_{14}mim^+$ at r = 2 in 50 mM NaCl solution at pH 7. The presence of SCX6 causes about 48-fold diminution in cac. $C_{14}mim^+$ association into micelles begins at 0.72 mM under analogous experimental conditions (50 mM NaCl). The binding to SCX6 polyanion lessens the electrostatic repulsion among the imidazolium headgroups of $C_{14}mim^+$ and promotes the self-organization of the alkyl chains thereby facilitating SM formation. The experiment was repeated in 30 and 75 mM NaCl solutions at r = 2. The cac value insignificantly altered with NaCl concentration. When 50 mM NaCl concentration was kept constant and [$C_{14}mim^+$]:[SCX6] ratio was varied, cac remained about 0.015 mM at r = 1, 2, 3 and 3.6 molar ratios alike.

The marked hypsochromic shift of the spectra upon inclusion in SM implies that HONR is situated in a microenvironment of moderate polarity where it is less accessible to interaction with water. Figure S2 in Supporting Information displays the change of the fluorescence maximum of HONR with the $E_T(30)$ solvent polarity parameter.[32,34] The data measured in neat solvents are fitted with a polynom. The obtained function serves as a calibration for the characterization of the surroundings around the dye in micelles. The

triangles indicate the substantial diminution of the local polarity compared to that in water. HONR senses microenvironment of 189 and 225 kJ $mol^{-1}$ $E_T(30)$ values in SM and $C_{14}mim^+$ micelle in 50 mM NaCl solution, respectively. The latter quantity corresponds to that reported for HONR bound to $C_{14}mim^+$ micelle in the absence of NaCl.[30] The surroundings of HONR were also insensitive to NaCl concentration in SMs. On the basis of the derived $E_T(30)$ parameters we conclude that the environment around the probe in $C_{14}mim^+$ micelle closely resembles that of diethylene glycol, whereas in SM the polarity is lower, and similar to that of dimethylformamide and acetonitrile. The binding site in SM provides larger protection against water compared to that in conventional $C_{14}mim^+$ micelle.

**Isothermal titration calorimetry (ITC).** To get insight into the thermodynamics of the association processes, ITC measurements were performed. A solution of 3.4 mM $C_{14}mim^+$ with 15 mM NaCl was injected into 0.1 mM SCX6 and 15 mM NaCl mixture at pH 7. The dilution heat of the titrant, which was determined by the titration of 15 mM NaCl, was always

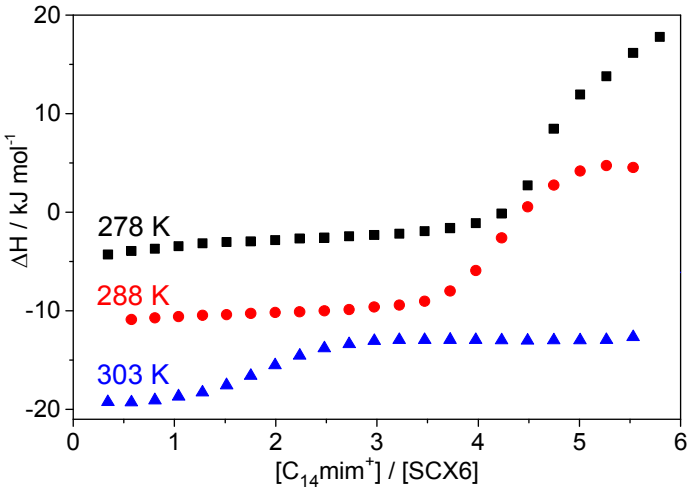


**Figure 7** Enthalpograms after correction with the dilution heat of the titrant solution at various temperatures. 3.4 mM $C_{14}mim^+$ solution was added to 0.1 mM SCX6 keeping 15 mM NaCl concentration constant.

subtracted. Representative results are presented in Figure 7, whereas enthalpograms at 0 and 50 mM NaCl concentrations are displayed in Supporting Information Figure S3 and S4. Figure S5 demonstrates that the same enthalpy gain is obtained irrespective of whether the concentration of $C_{14}mim^+$ is above or below cmc in the titrant solution. The heat evolution at low $C_{14}mim^+$:SCX6 ratios ($\Delta H_{SM}$) in 15 mM NaCl solution (Figure 7) is due to formation of inclusion complexes and self-assembly to SM. These two types of processes cannot be separated due to the small critical aggregation concentration (cac) of SMs. Since the heat evolution is constant at low ratios, this indicates that SMs are already formed after the first $C_{14}mim^+$ addition, showing that cac are very low (lower than 0.04 mM $C_{14}mim^+$ in 0.1 mM SCX6). This is in accordance with the 0.015 mM cac of $C_{14}mim^+$ in 0.1 mM SCX6 determined by HONR fluorescence probe (vide supra). At 278 and 288 K, the consecutive injections at low [$C_{14}mim^+$]:[SCX6] ratios increase only the number of SMs, therefore the produced heat barely varies. At larger [$C_{14}mim^+$]:[SCX6] ratios, the enthalpy change becomes less negative or even positive because of the transformation of SMs to NPs. The shift of the inflexion point of the enthalpograms (Figure 7) indicates that smaller amount of $C_{14}mim^+$ is sufficient to induce SM–NP conversion at higher temperature. The plateau of the sigmoid curves at large [$C_{14}mim^+$]:[SCX6] ratios corresponds to the enthalpy of NP formation ($\Delta H_{NP}$). The endothermic association to NPs at low temperature turns into exothermic above 292 K, whereas the enthalpy of SM formation from the components is always negative and diminishes with the increase of temperature. Figure 8A presents the temperature dependence of $\Delta H_{SM}$ and $\Delta H_M$, the enthalpy of $C_{14}mim^+$ conventional micelle formation, at 15 and 50 mM NaCl concentrations. $\Delta H_M$ was calculated from the results of the titration of NaCl solution with 20 mM $C_{14}mim^+$ as described by Blume and coworkers.[35] The enthalpy changes showed linear correlations with temperature, and the slopes provided the molar heat capacity changes ($\Delta C_p$). Neither $\Delta H_M$ nor $\Delta H_{SM}$ displayed NaCl concentration

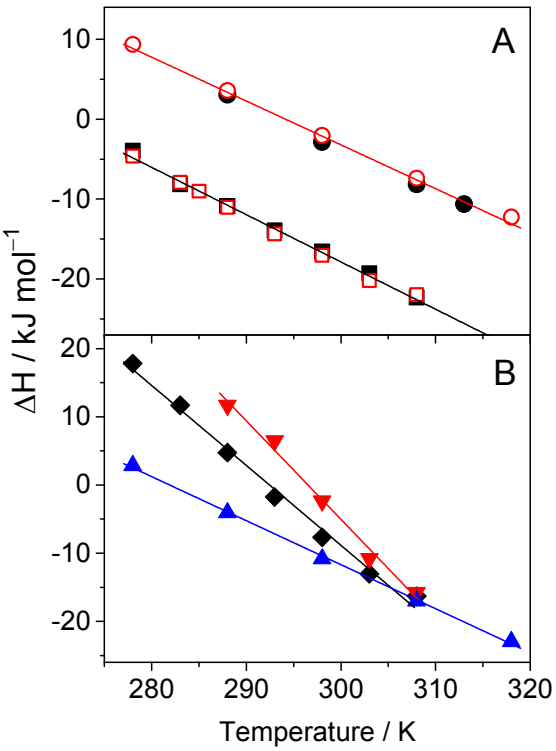


**Figure 8** Enthalpy changes per mole of $C_{14}mim^+$ as a function of temperature (A) for $C_{14}mim^+Br^-$ micelle (circles) and SM (squares) formation in 15 mM (filled symbols) and 50 mM (empty symbols) NaCl solution; (B) for NP formation in 0 (▲), 15 (♦), and 50mM (▼) NaCl solution.

influence on their temperature dependence. The increase of NaCl concentration from 15 to 50 mM did not modify the temperature dependence of $\Delta H_M$ and $\Delta H_{SM}$. The latter quantity is negative in the whole temperature range and about 14 kJ $mol^{-1}$ smaller than the enthalpy change of the conventional $C_{14}mim^+$ micelle formation. As seen in Table 1, the $\Delta C_p$ values for conventional and supramolecular micelles barely differ, and are in accordance with that reported for $C_{14}mim^+Cl^-$ micelle in neat water.[36] In contrast to the behavior of $\Delta H_{SM}$, a steeper and NaCl concentration sensitive temperature dependence was obtained for $\Delta H_{NP}$ (Figure 8B). $\Delta C_p$ of NP formation significantly decreased upon gradual increase of NaCl concentration.

**Table 1** Results of the linear least-squares fit of the temperature dependence of enthalpy changes

| Particle | [NaCl] / mM | $\Delta C_p$ / kJ mol$^{-1}$ K$^{-1}$ | Intercept / kJ mol$^{-1}$ |
|---|---|---|---|
| $C_{14}mim^+Cl^-$ micelle[a] | 0 | –0.595[a] | - |
| $C_{14}mim^+Br^-$ micelle | 15 | -0.54 | 161 |
| $C_{14}mim^+Br^-$ micelle | 50 | -0.54 | 160 |
| SM | 15 | -0.59 | 160 |
| SM | 50 | -0.59 | 159 |
| NP | 0 | -0.64 | 182 |
| NP | 15 | -1.17 | 343 |
| NP | 50 | -1.44 | 428 |

[a] Reference[36]

Noteworthily, the reversible transformation between SM and NP became equi-enthalpic around 308 K at various NaCl concentrations. The more negative $\Delta C_p$ for the association to NP compared with that for SM formation significantly contributes to the temperature-switchable character of SM–NP transition.

## 4. DISCUSSION

Our results demonstrate that three parameters, the molar ratio of the components, temperature, and NaCl concentration determine that either NPs or SMs are formed as a result of the self-assembly of $C_{14}mim^+$ and SCX6 in neutral solution. Since the critical micelle concentration of $C_{14}mim^+$ is 2.5 mM in neat water at 298 K,[30] the ionic liquid cations do not aggregate in the absence of SCX6 under the experimental conditions of our studies. The negative logarithm of the acid dissociation constants ($pK_a$) of the phenolic OH groups in

SCX6 are 3.29, 4.91, and 12.5 in 0.1 M NaCl solution at 298 K, and they shift to lower value in the presence of organic cations.[37] Therefore, most of SCX6 hosts contain two phenolate moieties, and the macrocycle has 8 negative charges at pH 7. Our results have shown that in the conditions where SMs are formed, cac is very low ($[C_{14}mim^+] = 0.015$mM) and depends neither on the mixing ratio r nor on NaCl concentration. Moreover, SM size (d ~ 6 nm) and structure are also independent on these two parameters, as shown by ITC and DLS measurements. When NPs are formed, their stoichiometry is around 7 with a negative surface charge suggesting a partial neutralization of the SCX6 negative charges, whatever the mixing ratio and NaCl concentration are. Contrary to SMs, $\Delta C_p$ of NPs depend on the salt concentration (ITC, Figure 8). TEM images have shown spherical particles with inner structure composed of building blocks of 2 nm size. The main change going from NP to SM

**Scheme 3** Illustration of nanoparticle and supramolecular micelle formation[a]

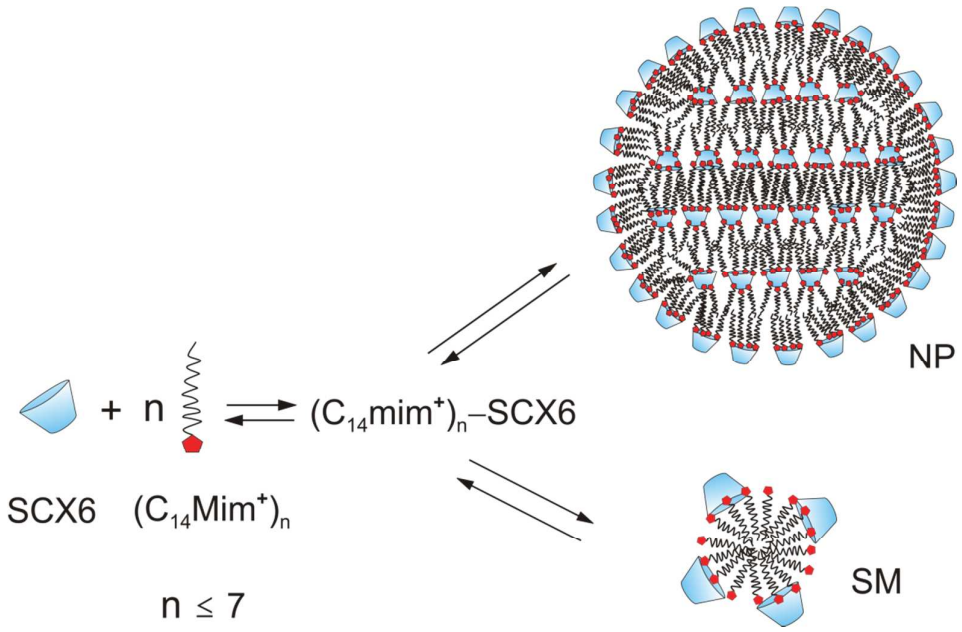


[a]In reality, the structure of SCX6 probably differs from the truncated cone shape. The counter-ions and charges were omitted for the sake of simplicity.

suspension is the large increase in the specific surface area of the particles. This could be a key parameter to understand the factors controlling the NP–SM transition.

Scheme 3 outlines NP and SM formations. Below cac, 1:1 complexation occurs between $C_{14}mim^+$ and SCX6. The equilibrium constant of this process (K) can be estimated on the basis of the K values published for the association of various 1-alkyl-3-methylimidazolium ($C_nmim^+$) with SCX6.[27] The extrapolation of the K dependence on the number of carbon atoms in $C_nmim^+$ with a second order polynom provided $K = 1.9\times10^4\ M^{-1}$ for the 1:1 inclusion of $C_{14}mim^+$ in SCX6 cavity. Multiple binding of $C_{14}mim^+$ to SCX6 macrocycle could also take place due to the electrostatic, host-guest and hydrophobic interactions producing $(C_{14}mim^+)_n$–SCX6. Above cac, the $(C_{14}mim^+)_n$–SCX6 complexes aggregate either to NPs or SMs depending on the experimental conditions. The reversible transformation between NP and SM probably also occurs via $(C_{14}mim^+)_n$–SCX6. Only NPs or SMs were observed experimentally.

The NP–SM transition is markedly influenced by the NaCl concentration (Figure 1 and 2). This salt effect may arise from several factors. (i) $Na^+$ cations can competitively bind to the macrocycle. DOSY NMR measurements showed $Na^+$ association with SCX6.[38] The analogous reaction of $Na^+$ with the smaller homologue, 4-sulfonatocalix[4]arene, has a low association constant[39] of 183 $M^{-1}$. This is probably not a predominant process. (ii) $Na^+$ ions can screen the electrostatic repulsion among negatively charged species promoting thereby their colloidal destabilization. This is observed for NPs at mixing ratios of 5 and 6. At lower mixing ratios, the observed NP–SM transformation cannot be explained by screening effect. (iii) $Na^+$ and $Cl^-$ ions may interact with the first hydratation shell of the ionic moieties and interfere with the ordered hydrate structure around the hydrophobic chains. (iv) $Na^+$ cations can serve as loosely bound counterions for SM and NP alike. Adsorption of counterions in the Stern layer could partly explain the NP–SM transition. Because of the surface area

difference, the number of bound cations should be much higher for SMs than for NPs at large salt concentration where saturation of $Na^+$ adsorption occurs.

The transition between SMs and NPs also depends on the temperature and the mixing ratio r at a given salt concentration. Due to the negative $\Delta H_{SM}$ and the endothermic character of the self-assembly to NP (Figure 8), SM formation prevails at low temperature. The more negative $\Delta C_p$ renders the enthalpy of NP formation more temperature sensitive than that of SM production. Therefore, NP formation becomes energetically favorable at high temperature and mixing ratio. From the comparison of the data in Figure 7 and 8, we conclude that NP can be formed even when $\Delta H_{NP}$ is positive. This indicates the substantial favorable entropy contribution to the driving force. The entropy increase arising from the release of water molecules from the ordered hydrate structure around the individual hydrophobic carbon chains[40] and from the solvate shell of the ionic moieties[39] is only partly compensated by the entropy diminution due to association into NPs. As the temperature is raised, the ordered aqueous region surrounding the aliphatic groups gradually vanishes and the extent of hydration around the ionic groups diminishes leading to lessening entropy gain for NP formation. The barely different $\Delta C_p$ for conventional $C_{14}mim^+$ micelles and SMs indicates that the hydrophobic molecular surface exposed to water is the dominant factor determining $\Delta C_p$.[36] The presence of SCX6 in the headgroup region barely alters the degree of water penetration into the micelles.

## 5. CONCLUSIONS

Inclusion complex formation promotes the self-organization of $C_{14}mim^+$ and SCX6 ions either to NP or SM in neutral solutions depending on temperature, mixing ratio of the component and NaCl concentration. SMs are formed in an exothermic and practically NaCl concentration independent process above 0.015 mM critical aggregation concentration. They

are stable only in the presence of NaCl, at low temperature, and at $[C_{14}mim^+]$:[SCX6] $\leq$ 4 mixing ratios. Otherwise spherical NP production has a larger driving force. At low temperature, NPs do not exist because the entropy gain cannot overcompensate the endothermicity of their formation. The salt sensitive and substantially negative molar heat capacity change upon self-assembly to NPs plays important role in determining the conditions for NP stability. The reversible SM–NP transformation may find applications in systems possessing thermally switchable optical properties and in stimuli-responsive assemblies capable of controlled release of substrates.

**Supporting Information**

Figures S1 – S5. This material is available free of charge via the Internet at http://pubs.acs.org.

**Acknowledgment**

We appreciate the support of this work by the Hungarian Scientific Research Fund (OTKA, Grant K104201) and the bilateral program between CNRS and the Hungarian Academy of Sciences. Z. M. thanks the support of the János Bolyai Research Scholarship of the Hungarian Academy of Sciences.

**References**

(1) Kang, Y.; Liu, K.; Zhang, X. Supra-Amphiphiles: A New Bridge between Colloidal Science and Supramolecular Chemistry. *Langmuir* **2014**, *30*, 5989-6001.

(2) Zhang, X.; Wang, C. Supramolecular Amphiphiles. *Chem. Soc. Rev.* **2011**, *40*, 94-101.

(3) Xing, P.; Sun, T.; Hao, A. Vesicles from Supramolecular Amphiphiles. *RSC Adv.* **2013**, *3*, 24776-24793.

(4) Valente, A. J. M.; Söderman, O. The Formation of Host–Guest Complexes between Surfactants and Cyclodextrins. *Adv. Colloid Interface Sci.* **2014**, *205*, 156-176.

(5) Jiang, L.; Deng, M.; Wang, Y.; Liang, D.; Yan, Y.; Huang, J. Special Effect of β-Cyclodextrin on the Aggregation Behavior of Mixed Cationic/Anionic Surfactant Systems. *J. Phys. Chem. B* **2009**, *113*, 7498-7504.

(6) Jeon, Y. J.; Bharadwaj, P. K.; Choi, S.; Lee, J. W.; Kim, K. Supramolecular Amphiphiles: Spontaneous Formation of Vesicles Triggered by Formation of a Charge-Transfer Complex in a Host. *Angew. Chem. Int. Ed.* **2002**, *41*, 4474-4476.

(7) Jiao, D.; Geng, J.; Loh, X. J.; Das, D.; Lee, T.-C.; Scherman, O. A. Supramolecular Peptide Amphiphile Vesicles through Host–Guest Complexation. *Angew. Chem. Int. Ed.* **2012**, *51*, 9633-9637.

(8) Versluis, F.; Tomatsu, I.; Kehr, S.; Fregonese, C.; Tepper, A. W. J. W.; Stuart, M. C. A.; Ravoo, B. J.; Koning, R. I.; Kros, A. Shape and Release Control of a Peptide Decorated Vesicle through Ph Sensitive Orthogonal Supramolecular Interactions. *J. Am. Chem. Soc.* **2009**, *131*, 13186-13187.

(9) Yan, Q.; Yuan, J.; Cai, Z.; Xin, Y.; Kang, Y.; Yin, Y. Voltage-responsive Vesicles Based on Orthogonal Assembly of Two Homopolymers. *J. Am. Chem. Soc.* **2010**, *132*, 9268-9270.

(10) Zhang, J.; Shen, X. Temperature-induced Reversible Transition between Vesicle and Supramolecular Hydrogel in the Aqueous Ionic Liquid−β-Cyclodextrin System. *J. Phys. Chem. B* **2013**, *117*, 1451-1457.

(11) Nalluri, S. K. M.; Voskuhl, J.; Bultema, J. B.; Boekema, E. J.; Ravoo, B. J. Light-responsive Capture and Release of DNA in a Ternary Supramolecular Complex. *Angew. Chem. Int. Ed.* **2011**, *50*, 9747-9751.

(12) Wang, Y.; Ma, N.; Wang, Z.; Zhang, X. Photocontrolled Reversible Supramolecular Assemblies of an Azobenzene-containing Surfactant with α-Cyclodextrin. *Angew. Chem. Int. Ed.* **2007**, *46*, 2823-2826.

(13) Atwood, J. L.; Barbour, L. J.; Hardie, M. J.; Raston, C. L. Metal Sulfonatocalix[4,5]arene Complexes: Bi-layers, Capsules, Spheres, Tubular Arrays and Beyond. *Coord. Chem. Rev.* **2001**, *222*, 3-32.

(14) Qin, Z.; Guo, D. S.; Gao, X. N.; Liu, Y. Supra-amphiphilic Aggregates Formed by *p*-Sulfonatocalix[4]arenes and the Antipsychotic Drug Chlorpromazine. *Soft Matter* **2014**, *10*, 2253-2263.

(15) Ling, I.; Alias, Y.; Raston, C. L. Structural Diversity of Multi-component Self-assembled Systems Incorporating *p*-Sulfonatocalix[4]arene. *New J. Chem.* **2010**, *34*, 1802-1811.

(16) Guo, D.-S.; Liu, Y. Supramolecular Chemistry of *p*-Sulfonatocalix[n]arenes and Its Biological Applications. *Acc. Chem. Res.* **2014**, *47*, 1925-1934.

(17) Perret, F.; Lazar, A. N.; Coleman, A. W. Biochemistry of the *para*-Sulfonatocalix[n]arenes. *Chem. Commun.* **2006**, 2425-2438.

(18) Perret, F.; Coleman, A. W. Biochemistry of Anionic Calix[n]arenes. *Chem. Commun.* **2011**, *47*, 7303-7319.

(19) Danylyuk, O.; Suwinska, K. Solid-State Interactions of Calixarenes with Biorelevant Molecules. *Chem. Commun.* **2009**, 5799–5813.

(20) Guo, D.-S.; Liu, Y. Calixarene-based Supramolecular Polymerization in Solution. *Chem. Soc. Rev.* **2012**, *41*, 5907-5921.

(21) Gadde, S.; Batchelor, E. K.; Weiss, J. P.; Ling, Y.; Kaifer, A. E. Control of H- and J-Aggregate Formation via Host−Guest Complexation Using Cucurbituril Hosts. *J. Am. Chem. Soc.* **2008**, *130*, 17114-17119.

(22) Megyesi, M.; Biczók, L. Considerable Change of Fluorescence Properties upon Multiple Binding of Coralyne to 4-Sulfonatocalixarenes. *J. Phys. Chem. B* **2010**, *114*, 2814-2819.

(23) Basilio, N.; Martín-Pastor, M.; García-Río, L. Insights into the Structure of the Supramolecular Amphiphile Formed by a Sulfonated Calix[6]arene and Alkyltrimethylammonium Surfactants. *Langmuir* **2012**, *28*, 6561-6568.

(24) Lau, V.; Heyne, B. Calix[4]arene Sulfonate as a Template for Forming Fluorescent Thiazole Orange H-Aggregates. *Chem. Commun.* **2010**, *46*, 3595-3597.

(25) Basílio, N.; Piñeiro, Á.; Da Silva, J. P.; García-Río, L. Cooperative Assembly of Discrete Stacked Aggregates Driven by Supramolecular Host–Guest Complexation. *J. Org. Chem.* **2013**, *78*, 9113-9119.

(26) Miskolczy, Z.; Biczók, L. Inclusion Complex Formation of Ionic Liquids with 4-Sulfonatocalixarenes Studied by Competitive Binding of Berberine Alkaloid Fluorescent Probe. *Chem. Phys. Lett.* **2009**, *477*, 80-84.

(27) Wintgens, V.; Biczók, L.; Miskolczy, Z. Thermodynamics of Host-Guest Complexation between *p*-Sulfonatocalixarenes and 1-Alkyl-3-Methylimidazolium Type Ionic Liquids. *Thermochim. Acta* **2011**, *523*, 227-231.

(28) Wintgens, V.; Amiel, C.; Biczók, L.; Miskolczy, Z.; Megyesi, M. Host–Guest Interactions between 4-Sulfonatocalix[8]arene and 1-Alkyl-3-Methylimidazolium Type Ionic Liquids. *Thermochim. Acta* **2012**, *548*, 76-80.

(29) Wintgens, V.; Le Coeur, C.; Amiel, C.; Guigner, J. M.; Harangozó, J. G.; Miskolczy, Z.; Biczók, L. 4-Sulfonatocalix[6]arene-Induced Aggregation of Ionic Liquids. *Langmuir* **2013**, *29*, 7682-7688.

(30) Vanyúr, R.; Biczók, L.; Miskolczy, Z. Micelle Formation of 1-Alkyl-3-Methylimidazolium Bromide Ionic Liquids in Aqueous Solution. *Colloids Surfaces A: Physicochem. Eng. Aspects* **2007**, *299*, 256-261.

(31) Yang, W.; Villiers, M. M. d. The Solubilization of the Poorly Water Soluble Drug Nifedipine by Water Soluble 4-Sulphonic Calix[n]arenes. *Eur. J. Pharm. Biopharm.* **2004**, *58*, 629–636.

(32) Nagy, K.; Göktürk, S.; Biczók, L. Effect of Microenvironment on the Fluorescence of 2-Hydroxy-Substituted Nile Red Dye: A New Fluorescent Probe for the Study of Micelles. *J. Phys. Chem. A* **2003**, *107*, 8784-8790.

(33) Miskolczy, Z.; Sebők-Nagy, K.; Biczók, L.; Göktürk, S. Aggregation and Micelle Formation of Ionic Liquids in Aqueous Solution. *Chem. Phys. Lett.* **2004**, *400*, 296-300.

(34) Reichardt, C. Solvatochromic Dyes as Solvent Polarity Indicators. *Chem. Rev.* **1994**, *94*, 2319-2358.

(35) Paula, S.; Sues, W.; Tuchtenhagen, J.; Blume, A. Thermodynamics of Micelle Formation as a Function of Temperature: A High Sensitivity Titration Calorimetry Study. *J. Phys. Chem.* **1995**, *99*, 11742-11751.

(36) Gilani, A. G.; Moghadam, M.; Hosseini, S. E.; Zakerhamidi, M. S. A Comparative Study on the Aggregate Formation of Two Oxazine Dyes in Aqueous and Aqueous Urea Solutions. *Spectrochimica Acta - Part A: Molecular and Biomolecular Spectroscopy* **2011**, *83*, 100-105.

(37) Suga, K.; Ohzono, T.; Negishi, M.; Deuchi, K.; Morita, Y. Effect of Various Cations on the Acidity of *p*-Sulfonatocalixarenes. *Supramol. Sci.* **1998**, *5*, 9-14.

(38) Basilio, N.; García-Río, L.; Martín-Pastor, M. Counterion Binding in Solutions of *p*-Sulfonatocalix[4]arene. *J. Phys. Chem. B* **2010**, *114*, 7201-7206.

(39) Francisco, V.; Piñeiro, A.; Nau, W. M.; García-Río, L. The "True" Affinities of Metal Cations to *p*-Sulfonatocalix[4]arene: A Thermodynamic Study at Neutral pH Reveals a Pitfall Due to Salt Effects in Microcalorimetry. *Chem. Eur. J.* **2013**, *19*, 17809-17820.

(40) Bordello, J.; Reija, B.; Al-Soufi, W.; Novo, M. Host-Assisted Guest Self-Assembly: Enhancement of the Dimerization of Pyronines Y and B by γ-Cyclodextrin. *ChemPhysChem* **2009**, *10*, 931-939.

## Table of contents graphic